Lithos 318–319 (2018) 219–229

Contents lists available at ScienceDirect

Lithos

journal homepage: www.elsevier.com/locate/lithos

# Ediacaran to lower Cambrian basement in eastern George V Land (Antarctica): Evidence from U—Pb dating of gneiss xenoliths and implications for the South Australia- East Antarctica connection

Gaëlle Lamarque [a,b,*], Jérôme Bascou [a], René-Pierre Ménot [a], Jean-Louis Paquette [c], Simon Couzinié [d], Yann Rolland [e], Jean-Yves Cottin [a]

[a] Université de Lyon, UJM Saint-Etienne, UMR CNRS IRD 6524, Laboratoire Magmas et Volcans, F-42023 Saint-Etienne, France
[b] Ifremer, Geosciences Marines, Centre de Brest, 29280 Plouzané, France
[c] UMR CNRS IRD 6524, Laboratoire Magmas et Volcans, 63038 Clermont-Ferrand, France
[d] Université de Lyon, ENSL, UCBL, CNRS,LGL-TPE, 69007 Lyon, France
[e] Université de Nice-Sophia Antipolis, Géoazur, UMR CNRS 7329, 250 rue Albert Einstein, 06560 Valbonne, France

ARTICLE INFO

*Article history:*
Received 4 June 2018
Accepted 15 August 2018
Available online 20 August 2018

*Keywords:*
Gondwana margin
Ross orogeny
George V Land
Antarctica-Australia connection
Zircon and monazite U—Pb dating

ABSTRACT

This study presents the first geochronological results on basement rocks from the Penguin-Bage-Webb (PBW) domain located east of the Neoarchean-Paleoproterozoic Terre Adélie craton, Antarctica. Investigated samples are paragneiss xenoliths hosted within early Paleozoic granitoids, which were emplaced during the Ross orogeny. Zircon U—Pb dating yielded ages ranging from the Archean to the Cambrian, with a dominant Ediacaran (550–635 Ma) population and maximum depositional ages around 570–575 Ma. U–Th–Pb analyses of monazite suggest that the metamorphic event that formed the gneiss samples occured at ca. 515 Ma, shortly prior to incorporation within the granitic magmas. The studied samples likely represent relics of the pre-Gondawana Pacific margin, which was subsequently deformed and metamorphosed during the early Paleozoic Ross orogeny. The obtained zircon U—Pb date distributions present similarities with those of the Kanmantoo and Nargoon sediments in Southern Australia and provide new constrains for the correlations between East Antarctica and South Australia before the opening of the Southern Ocean.



## 1. Introduction

The initial configuration of Gondwana and its fragmentation are still debated because of the lack of consensus on the nature of major structures and geological domains that composed the super-continent. In East Gondwana, the region of Terre Adélie and George V Land (East Antarctica) is considered to represent southern extension of South Australia (Borg and Depaolo, 1994; Di Vincenzo etal., 2014; Flöttmann etal., 1993; Oliver and Fanning, 1997; Payne etal., 2009; Peucat etal., 1999, 2002; Reading, 2004; Talarico and Kleinschmidt, 2003a), Fig. 1. In particular, the continuity of the Terre Adélie Craton in Antarctica with the western Gawler Craton (Australia), both being parts of the Neoarchean-Paleoproterozoic Mawson Continent, is well documented from geological (Fanning etal., 1999, 2003; Fitzsimons, 2003) and geophysical studies (Aitken etal., 2014). However, the continuity of the domains located east of the Mawson Continent needs to be refined because lacks and inconsistencies exist. For example, outcrops from the eastern Gawler Craton (Australia) characterized by 1.85 and 2.0 Ga ages (Hand etal., 2007), as well as Ediacaran-early Cambrian formations such as Kanmantoo group (Ireland etal., 1998) do not display correlatives neither in eastern George V Land (Antarctica) nor in the Terre Adélie Craton. Furthermore, the lack of geochronological data from eastern George V Land, more specifically on the Penguin-Bage-Webb block (close to the Terre Adélie Craton), is a key issue to better understand the Precambrian connections between Australia and Antarctica and subsequently the evolution of both the Mawson Continent and the Gondwana.

The aim of this contribution is thus to constrain the age of the Penguin-Bage-Webb basement block located east of the Terre Adélie Craton and separated from it by the Mertz Shear Zone (Di Vincenzo etal., 2007; Ménot etal., 2007). Up to now, only the cross-cutting granitoids of Penguin Point have been dated by zircon U—Pb analyses at 505 Ma (Fanning etal., 2002) and 508–510 ± 5 Ma (Goodge and Fanning, 2010), and by biotite $Ar^{39}/Ar^{40}$ analyses at 487.7 ± 3.5 Ma (Di

* Corresponding author.
*E-mail address:* gaelle.lamarque@ifremer.fr (G. Lamarque).

https://doi.org/10.1016/j.lithos.2018.08.021
0024-4937/

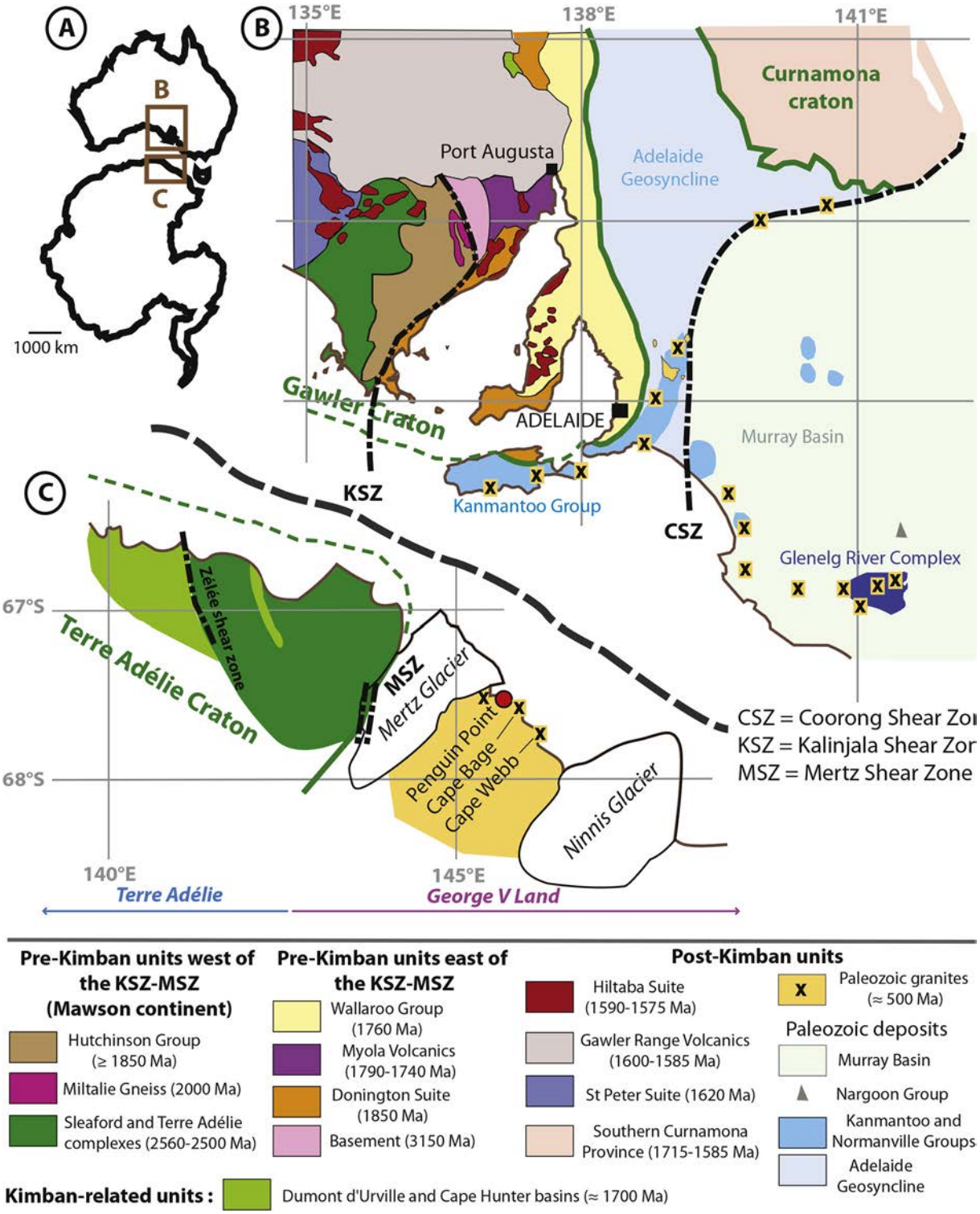


**Fig.1.** A) General map of Antarctica and Australia. B)Simplified geological map of the Gawler Craton and juxtaposed terrains (modified from Foden etal., 2002; Haines etal., 2009; Howard etal., 2006; Milnes etal., 1977; Reid etal., 2014). C)Synthetic geological map of study area, modified from Ménot etal. (2005). The green area represents the Terre Adélie Craton, whereas the yellow area is related to the Ross orogeny. The red circle represents the studied outcrop (Penguin Point). Note that the geological maps of south Australia and Terre Adélie-George VLand (B and C)are juxtaposed for graphical purpose but this is not representative of any paleo-reconstruction. (For interpretation of the references to colour in this figure legend, the reader is referred to the web version of this article.)

Vincenzo etal., 2007). The existence of gneiss xenoliths within the early Paleozoic granites offers a unique opportunity to clarify the age and nature of the underlying basement which have, up to now, never been addressed. In this study, we report the results of zircon and monazite U—Pb analyses performed on three gneiss xenoliths. The obtained datasetallows to discuss: (i)the potential extension of the Terre Adélie Craton eastward and the role of the Mertz Shear Zone to the tectonic evolution of the area, and, (ii) the correlation between the Penguin-Bage-Webb block and its presumably corresponding Australian formations.

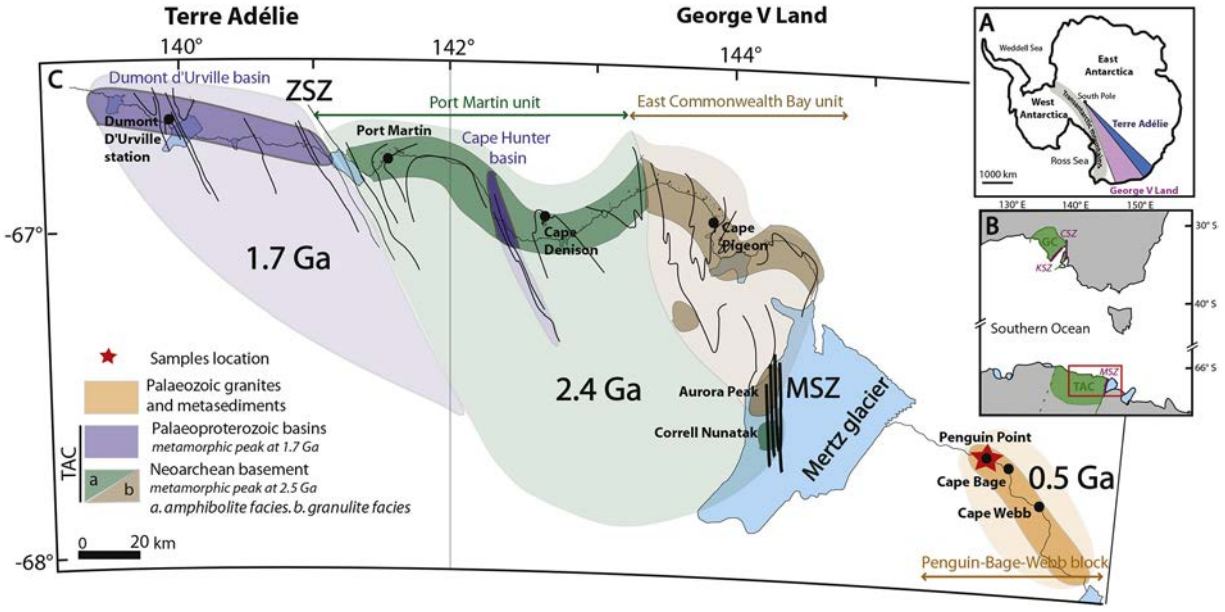


**Fig.2. A:** Location of Terre Adélie and George V Land in the Antarctic continent. **B:** Link between south Australia and Antarctica. TAC = Terre Adélie Craton, GC = Gawler Craton, MSZ= Mertzshear zone, KSZ = Kalinjala shear zone, CSZ = Coorong shear zone. **C:** Synthetic geological map of the Terre Adélie Craton (after Ménot etal., 2007). Purple areas are Paleoproterozoic terrains, which correspond to the Dumont d'Urville and Cape Hunter basins; green and brown areas are Neoarchean terrains, green being intermediate to upper amphibolitic crust and brown granulite facies crust. Orange area represents the Paleozoic crust, mainly composed of granitoids. Darkest colours correspond to outcrops. MSZ denotes the Mertz shear zone and ZSZ denotes the Zélée shear zone. Directions of field-measured structures are drawn in black. Locations of studied samples are marked by red stars. See also Ménot etal. (2007) and Ménot (2018) for more complete geological description. (For interpretation of the references to colour in this figure legend, the reader is referred to the web version of this article.)

## 2. Geological setting

### 2.1. Terre Adélie and George V Land

The Terre Adélie and the western George V Land constitute the Terre Adélie Craton (135 to 145°E), which is part of the Neoarchean-Paleoproterozoic Mawson continent (Fanning etal., 2003). The Terre Adélie Craton is divided into two domains: the Neoarchean basement and the Paleoproterozoic metasedimentary basins (Ménot etal., 2007, see Figs. 1, 2). The Neoarchean basement (in green and brown on Fig.2) extends from 141°E (the Zélée shear zone, ZSZ) to 146°E (the MSZ) and is predominantly composed of felsic to mafic orthogneiss and granodiorites intruding siliciclastic metasediments with subordinate marbles and calc-silicates. This 2.55–2.44 Ga continental crust segment (Duclaux etal., 2008; Oliver and Fanning, 2002) exposes two distinct tectonic units that equilibrated under granulite and amphibolite facies conditions respectively, and then represent deep and intermediate crustal sections, respectively (Ménot etal., 2005). A thermal and tectonic event occurred at 1.7–1.5 Ga, as proposed by Di Vincenzo etal. (2007) on the basis of Ar/Ar dating. According to Duclaux etal. (2008), the 1.7 Ga event is likely to be restricted to narrow fluid-bearing anastomosed shear zones, concentrated on the edges of the Neoarchean domain (Mertz and Zélée shear zones). Synchronously to this event, the Paleoproterozoic metasedimentary basins were formed (purple in Fig. 2). They include the Dumont d'Urville (DDU) and Cape Hunter (CH) basins. DDU basin extends west from 141°E (the Zélée shear zone) and consists of dominant metapelitic migmatitic gneisses together with minor metagraywackes, silicic metavolcanics and mafic intrusions. The DDU formations experienced high-gradeamphibolite-facies metamorphic conditions (Pelletier etal., 2005). The CH basin appears as a tectonic unit within the Neoarchean basement and it mainly consists of phyllites equilibrated in greenschist-facies conditions (Ménot etal., 2005).

The exposed edge of the Terre Adélie Craton to the east is marked by the MSZ, which could correspond to the southern extension, on the Antarctica continent, of the Kalinjila or of the Coorong shear zones (Gawler Craton, south Australia) before the Cretaceous opening of the Southern Ocean (Gibson etal., 2013; Talarico and Kleinschmidt, 2003b). The MSZ is several km-wide, and bears a steeply-dipping pervasive mylonitic foliation and a subhorizontal to 20°north-plunging lineation with predominantly dextral motion indicators (Kleinschmidt and Talarico, 2000). This suggests that the MSZ might represent a mid-crustalstrike-slip fault that could have accommodated large horizontal displacements. Microstructural and thermo-barometric studies show that the MSZ deformation likely resulted in successive shear structures occurring under different metamorphic conditions from medium pressure amphibolite to greenschists facies up to 1.5 Ga (Duclaux etal., 2008; Lamarque etal., 2016; Talarico and Kleinschmidt, 2003b). Talarico and Kleinschmidt (2003a) highlighted undated brittle structures crosscutting the mylonic foliation and Ménot etal. (2005) suggest that a younger age (post-Ordovician?) cannot be formally ruled out because Paleozoic rocks are found to the East of the Mertz Glacier.

The domain east of the MSZ (145°E to 148°E, in yellow on Figs. 1 and2) corresponds to eastern George V Land and to the Penguin-Bage-Webb block. It is characterized by outcrops of granitoids with U—Pb dates of 505 Ma (Fanning etal., 2002) and 508–510 ± 5 Ma (Goodge and Fanning, 2010). Granites from Penguin Point display a large amount of gneiss and mafic microgranular xenoliths. They are massive with a mean grain size around 0.2–0.3 cm and they mainly contain quartz, feldspars and large flakes of biotite. Feldspars plagioclase is more abundant than K-feldspar. When compared to the descriptions of Ravich etal. (1968) given for the granites from the Ainsworth Bay (now Desolation Bay), the Penguin Point granites seem to be close to those of Cape Bage (located about 15 km away to East, see Fig. 1) and rather distinct to those of Cape Webb (more to the East, Fig. 1).

The studied samples occur as spherical to elongated xenoliths of fewtens of cm hosted within the Penguin Point granite (see xenoliths description in paragraph 3).

### 2.2. South Australia

A large part of South Australia corresponds to the Gawler Craton, which is also part of the Mawson continent (Fanning etal., 2003). The

Gawler Craton mainly consists of Archean to Paleoproterozoic basement that is overlain and intruded by Paleoproterozoic to Mesoproterozoic sedimentary, volcanic and intrusive rocks (Reid etal., 2014 and Fig. 1). The Archean basement is comprised of two temporally and spatially distinct pieces of crust that have unrelated formation and/or metamorphic histories. Mesoarchean (ca. 3250–3150 Ma) gneisses compose the oldest rocks, which are outcropping in the southeastern Gawler Craton (Reid etal., 2014, pink in Fig. 1). Neoarchean to earliest Paleoproterozoic domains include both the Sleaford Complex in the southern Gawler Craton (green in Fig. 1) and the Mulgathing Complex in the north central part of the craton that are composed of felsic, mafic and ultramafic volcanics as well as metasedimentary lithologies representing portions of a single Late Archean belt, deformed and metamorphosed during the Sleafordian Orogeny between 2450 and 2420 Ma (Daly and Fanning, 1993; Swain etal., 2005). The Miltalie gneiss intruded the Sleaford Complex during its uplift and erosion around 2000 Ma (Fanning etal., 1988; Fanning etal., 2007). Thereafter, the Hutchison Group (>1850 Ma) overlained the eastern margin of the Gawler Craton (Daly and Fanning, 1993). This group includes a basal quartz-pebble conglomerate and quartzite which change to calcareous and aluminous metasediments at the top (Parker and Lemon, 1982). The Hutchinson Group is limited to the east by a major tectonic structure, the Kalinjala shear zone (KSZ), formed during the ca. 1730–1690 Ma Kimban Orogeny. The Kimban Orogeny completed the volcano-sedimentary basin development during the Paleoproterozoic and extensively reworked the Archean and Paleoproterozoic domains through the activation of transpressional shear zones, such as the KSZ(Hand etal., 2007; Reid and Hand, 2012; Vassallo and Wilson, 2002). This later corresponds to a 4–6 km wide corridor showing subvertical mylonitic structures, associated magmatism as for example Middle Camp Granite and high-grade metamorphic assemblages (Parker, 1980; Vassallo and Wilson, 2002). However magmatic effect of the Kimban orogeny and relationships with large scale tectonic structures were mainly described across the central and northern Gawler craton (Hand etal., 2007). Thermal and mechanical effects of the high-strain zone activity could be observed in an area up to 100 km from the heart of the shear zone (see figure 5 of Hand etal., 2007). The KSZ likely represents a palaeosuture zone, separating two crustal (or possible lithospheric-scale) blocks with compositional differences (Howard etal., 2006). East of the Kalinjala shear zone, outcrops reveal the presence of a small area of felsic orthogneiss basement dated at 3150 Ma and deformed around 2530–2510 Ma (Fraser etal., 2010). This basement did not suffer any Sleafordian deformation. The Paleoproterozoic igneous Donington Suite (1850 Ma) intrudes sedimentary rocks with distinct isotopic signature from those located west of the Kalinjala shear zone (Howard etal., 2009). The Myola volcanics occurred between 1765 and 1735 Ma (Daly etal., 1998) and overly the Donington Suite. Following the Kimban Orogeny, magmatism took place during the time period 1690–1575 Ma. Markers of this magmatic activity include (i)the post-orogenic intrusive Tunkillia Suite (1690–1670 Ma), which origin is still debated (Payne etal., 2010), (ii) the voluminous St Peter Suite (1620–1610 Ma), which shows subduction origin (Hand etal., 2007; Swain etal., 2008) (iii) the Gawler Range Volcanics (1600–1585 Ma) which constitutes a silicic-dominated large igneous province (Agangi etal., 2011) and, (iv) the Hiltaba Suite (1590–1575 Ma) that developed into upper-crustal*syn*-tectonic plutons occuring in a wide zone of crustal shearing (McLean and Betts, 2003).

The Neoproterozoic to Paleozoic formations of South Australia are represented by the Adelaide Geosyncline (Fig. 1), which was fully described by Counts (2017). As a general overview, this rift complex is composed by successive (super)groups defined as (i)the Warrina supergroup which include both the Callanna group (minimum age around 802 ± 10 Ma) mainly composed of siltstone, sandstone, carbonates, evaporites and basalt; and the Burra group (~777–700 Ma) mainly consisting of siltstone, shale, sandstone and dolomite (Forbes etal., 1981; Krieg etal., 1991), (ii) the Heysen supergroup which include both the Umberatana group (~700–620 Ma) made up of tillite, sandstone, siltstone, arkose, dolomite, quartzite, conglomerate, shale and greywacke; and the Wilpena group (~588–566 Ma) mainly composed of siltstone with laminated quartzite, dolomite, marble and sandy marble (Knoll etal., 2006), and, (iii) the Moralana supergroup which include, among others, the Normanville (~526–515 Ma) made of limestone; sandstone; shale and volcanics; the Kanmantoo (~522–514 Ma) including marine metasandstone, phyllite, schist, gneiss, minor calcsilicate and marble; and the Lake Frome groups (~523–498 Ma) composed of sandstone, siltstone, shale, limestone and conglomerate (Zang etal., 2004). Study of detrital-zircon ages in the Adelaide fold belt (Ireland etal., 1998) shows an abrupt change in zircon population at the base of the Cambrian Kanmantoo Group. It is dominated by Ross-Delamerian (600–500 Ma) and Grenvillean ages (1200–1000 Ma) whereas zircons from Neoproterozoic sedimentary rocks (Normanville and older groups) mainly derived from the Australian cratons with ages progressively changing from Mesoproterozoic to Neoproterozoic and only few zircon that are close to the depositional age. Further east, the Murray Basin overlies these formations. The outcropping Glenelg River Complex (Fig. 1) as well as the Nargoon Group sampled from stratigraphic drill-hole, both within the Murray Basin, were described as correlative formations of Kanmantoo Group (Haines etal., 2009; Lewis etal., 2016, respectively). From geophysical data, Gibson etal. (2013) defined the previously unmapped Coorong Shear zone (see Fig. 1). The authors proposed that the Coorong shear zone represent the correlative structure of the Mertz shear zone located in Antarctica, as they are both aligned with the George V Land Facture Zone located in the Southern Ocean, thus challenging the generally accepted Kalinjala-Mertz correlation (Di Vincenzo etal., 2007; Kleinschmidt and Talarico, 2000; Talarico and Kleinschmidt, 2003a).

## 3. Sample description

We studied three gneiss samples hosted within the early Paleozoic granites of Penguin Point (146°E), which constitutes the westernmost outcrop of granites from Penguin-Bage-Webb area. The gneiss samples display sharp boundaries with the host granites (Fig. 3) and distinct petrographic features. Sample 12GL04 is a banded leucocratic gneiss with alternating centimetric thick (up to 5 cm) quartz-feldspar layers and thin (up to 2 mm) biotite beds. It could correspond to the “fine-grained feldspathic quartzite” described by Ravich etal. (1968). Sample 12GL01 is a homogeneous biotite -rich gneiss. Samples 12GL01 and 12GL04 display rather comparable textures and mineralogy. They mainly differ by the grain size of minerals (quartz, feldspars, biotite) being larger in 12GL01 than in 12GL04. They are granoblastic to grano-lepidoblastic with equigranular (0.2 to 0.3 mm-large in 12GL04 and 1.1 to 1.2 mm in 12GL01) undeformed quartz and feldspar mosaic suggesting a late static recrystallization which would be more developed in 12GL01 compared to 12GL04. Andesine plagioclase is more widely present than K-feldspar. Biotite flakes (0.2 to 1.2 mm-long) clearly mark the foliation; they enclose a lot of inclusions such as zircon and Fe-oxides (mainly ilmenite). Muscovite was occasionally observed.

Sample 12GL02 corresponds to a migmatitic gneiss with quartz-feldspar leucosomes occuring as lenses and small dykelets intruding the melanocratic layers, and presenting a granular texture. The melanocratic layers consist of poikiloblastic garnet crystals (up to several mm in size) that contain alignments of biotite and Fe-oxides, which consist of ilmenite grains generally elongated (up to 0.8 mm-long and 0.4 mm-wide). Thus, biotite and ilmenite mark a former foliation.

In all three samples, the zircon grains are mainly included within biotite crystals, but few occur as intergranular isolated grains within the matrix. The high modal proportion of biotite and the presence of garnet are consistent with a sedimentary origin for the protoliths, which likely corresponded to greywackes.

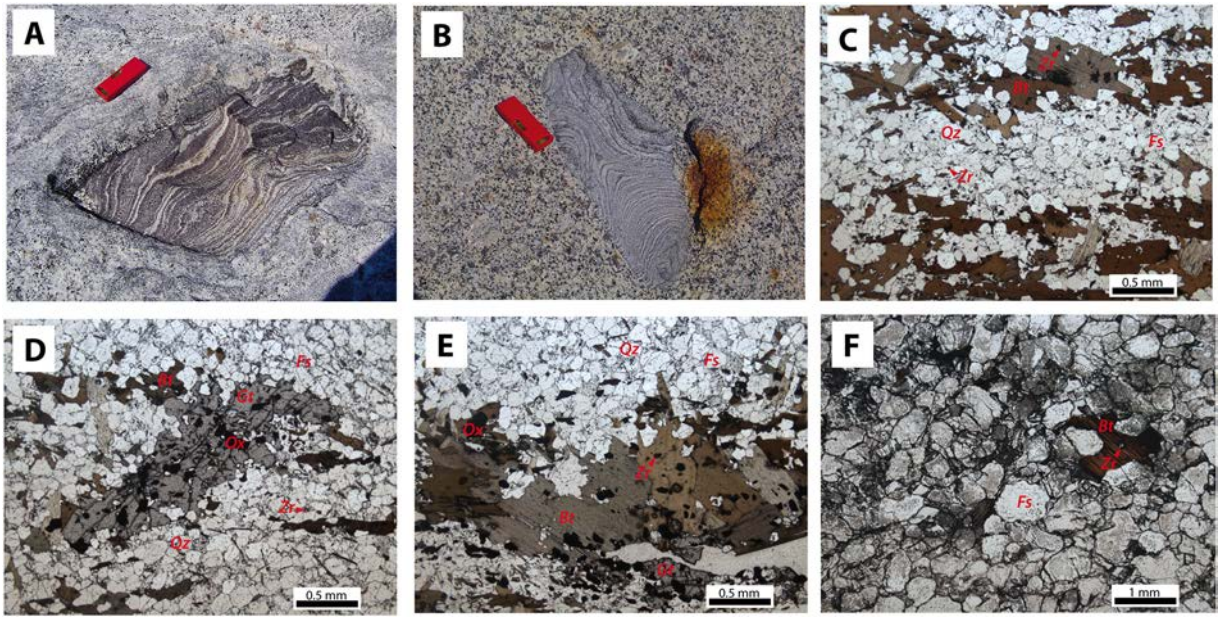


**Fig.3.** A, B)Photographs of xenoliths in the field, and their relations with the host granite. C)Thin-section photograph of sample 12GL01. D, E)Thin-section photograph of sample 12GL02. F) Thin-section photograph of sample 12GL04.

## 4. U—Pb zircon data

### *4.1. Analytical techniques and data processing*

Rock samples were crushed using standard procedure (jaw, crusher, disc mill) and sieved to <500 μm. Zircon and monazite grains were separated using heavy liquids, an isodynamic Frantz separator, and then handpicked under a binocular microscope to obtain a representative selection of all components present in the zircon population. Selected zircon grains were mounted in epoxy resin and polished to an equatorial grain section. Analytical work was carried out in the Laboratoire Magmas et Volcans (Clermont-Ferrand, France). Minerals were imaged by cathodoluminescence (CL) using a JEOLJSM-5910SEM to document their internal structure, resorption surfaces, and overgrowths (Hanchar and Miller, 1993; Vavra, 1990). The analyses involved the ablation of minerals with a Resonetics M-50 Excimer laser system operating at a wavelength of 193 nm. Spot diameters of 26 μm (zircon) and 9 μm (monazite) were associated to repetition rates of 3 Hz (zircon) and 1Hz (monazite) and fluency of 4.5 J/cm$^2$ (zircon) and 8 J/cm$^2$ (monazite). The ablated material was carried into helium and then mixed with nitrogen and argon before injection into the plasma source of an Agilent 7500cs ICP-MS(Paquette etal., 2014). The analytical method for isotope dating with laser ablation ICPMS is reported in (Hurai etal., 2010; Paquette etal., 2017). Data are corrected for U—Pb fractionation occurring during laser sampling and for instrumental mass bias by standard bracketing with repeated measurements of GJ-1 zircon standard (Jackson etal., 2004) and C83–32 monazite standard (Corfu, 1988). The occurrence of common Pb in the sample was monitored by the evolution of the $^{204}$(Pb + Hg) signal intensity, but no common Pb correction was applied owing to the large isobaric interference from Hg. Repeated analyses of 91,500 zircon (Wiedenbeck etal., 1995) and Trebilcock monazite (Kohn and Vervoort, 2008) standards treated as unknowns yielded concordia ages of 1067 ± 3 Ma ($MSWD_{(C+E)}$ = 0.45; $n$ = 69) and 271 ± 2 Ma ($MSWD_{(C+E)}$ = 1.2; $n$ = 20), independently control the reproducibility and accuracy of the corrections. Data reduction was carried out with the software package GLITTER® from Macquarie Research Ltd.(Van Achterbergh etal., 2001). Calculated ratios were exported and Concordia ages and diagrams were generated using Isoplot/Ex v. 3.7 Excel macro package by Ludwig (2008). The concentrations in U-Th-Pb were calibrated relative to the certified contents of GJ-1 zircon (Jackson etal., 2004) and Moacyr monazite (Gasquet etal., 2010) standards, respectively.

Results of U—Pb analyses for all samples are summarized in TableS1 (supplementary data).

### *4.2. Results*

Most zircon grains analyzed in the course of this study are light yellow, but a population of bigger dark brown grains was found in sample 12GL02, some of which being metamict. Cathodoluminescence images of representative grains are presented in Fig. 4. They are characterized by elliptical to rounded shapes (aspect ratio ranging from 0.3 to 1 with mean value of about 0.6). Core-rim relationships are common and most core and rim domains feature oscillatory to patchy zoning. Narrow CL-bright rims (<10 μm large) are also observed. Secondary textures include healed cracks and fractures. In some cases, only part of the zircon grain is preserved and do not show any core-rim structure. The variety of internal growth structures and the wide range of Th/U ratios between 0.01 and 5.78 support derivation from various igneous and/or metamorphic protoliths, consistent with a metasedimentary origin of the gneiss samples.

Results of zircon U—Pb dating are presented in Wetherill diagrams for each sample in Figs. 5a,b and 6a. Zircon date distributions are reported as Kernel Density Estimates (Fig.5e,f) following Vermeesch (2012). The comprehensive analytical dataset for all grains is provided in TableS1 (supplementary data). In the following, quoted dates are $^{206}$Pb/$^{238}$U dates when younger than 1.2 Ga. Otherwise, the $^{207}$Pb/$^{206}$Pb dates are preferred.

#### *4.2.1. Sample 12GL02*

A total of 76 U-Pb analyses were performed on 62 zircon grains. Sixty-two analyses are concordant at 90–110% (with concordance defined as $^{206}$Pb/$^{238}$U date/$^{207}$Pb/$^{206}$Pb date × 100). Following Vermeesch (2004), it entails that we can be confident at 95% that no fraction representing >8% of the sample has been missed. 12GL02 is typified by (i)a dominant Ediacaran (549–628 Ma) zircon population ($N$ = 27; Fig.5a,c,e); (ii) a subordinate population ($N$ = 4) with Cryogenian-late Tonian dates (693–784 Ma); (iii) grains yielding dates scattered between the early Tonian and the Stenian (0.9 to 1.2 Ga; $N$ = 10); (iv) an important Archean population ($N$ = 21), clustering at c. 2.7 and 3.1 Ga

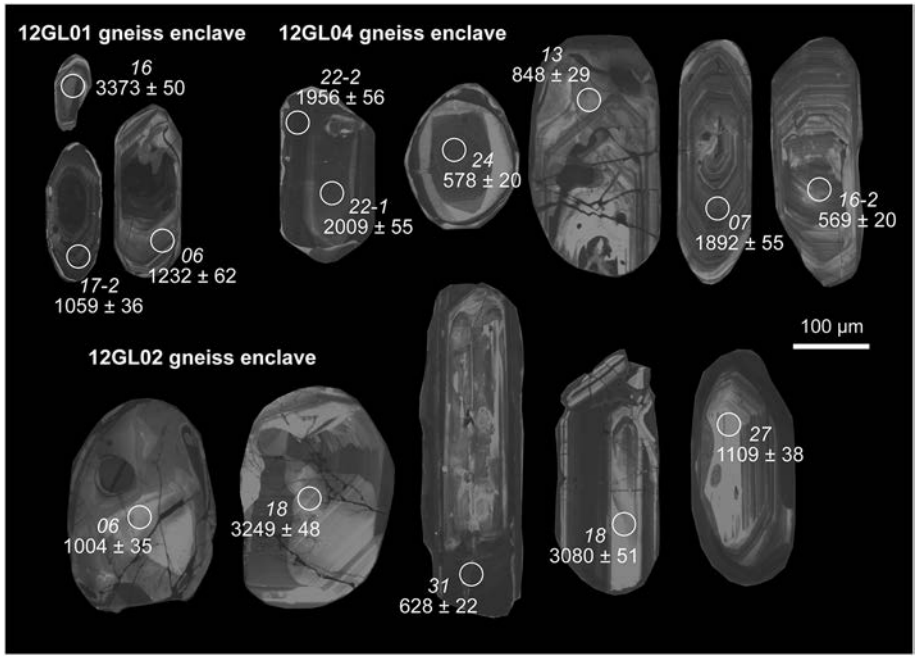


**Fig.4.** Cathodoluminescence images of selected zircon grains from paragneiss xenoliths 12GL01, 12GL02 and 12GL04. The circles represent the locations of laser spots and the obtained dates (in Ma) together with their uncertainties (at 2σ). $^{206}Pb/^{238}U$ dates are reported when younger than 1.2 Ga. For older dates, the $^{207}Pb/^{206}Pb$ dates are preferred. This applies to all figures in the contribution.

(Fig.5e). Besides, four discordant analyses show $^{207}Pb/^{206}Pb$ dates in excess of 2.6 Ga. Importantly, zircon grains showing Ediacaran and Archean dates display a very large range of Th/U ratios (from 0.01 to 2.39, Table S1) and textural patterns. In contrast, the early Tonian-Stenian population mostly consists of grains with oscillatory zoning textures and elevated Th/U ratios (mostly between 0.3 and 0.8, TableS1). The 16 youngest Ediacaran grains showing overlapping $^{206}Pb/^{238}U$ dates at 2σ allowed calculation of a weighted average date of 569.4 ± 5.0 Ma (Fig.5c). Finally, one single CL-dark, low Th/U (0.03) and U-rich (2600 ppm) zircon crystal yielded a Cambrian $^{206}Pb/^{238}U$ date of 514 ± 18 Ma.

*4.2.2. Sample 12GL04*

Thirty-four measurements were performed on 27 zircon grains and 23 yielded U—Pb dates concordant at 90–110%, meaning that no fraction representing >18% of the sample has been missed (at 95% confidence). Sample 12GL04 also features a dominant Ediacaran population (569–622 Ma, $N = 9$, Fig.5b,d,f) with again a large variety of internal growth structures and a wide range of Th/U ratios between 0.11 and 5.78 (Table S1). Two grains yielded Tonian dates of 848 ± 29 and 910 ± 31 Ma. One grain show a date of 1200 ± 40 Ma, i.e. at the Stenian-Ectasian boundary. Notably, 12GL04 differs from 12GL02 by the presence of a Paleoproterozoic zircon population defining sub peaks at c. 1.9 and 2.4 Ga ($N = 5$). Grains of that age feature oscillatory zoning patterns and a narrow range of Th/U ratios (0.33 to 0.52, Table S1). One grain has the oldest concordant $^{207}Pb/^{206}Pb$ date retrieved in the course of this study (at 3.4 Ga). Finally, a weighted average date of 575.2 ± 8.3 Ma can be calculated considering the 6 youngest Ediacaran grains showing overlapping $^{206}Pb/^{238}U$ dates at 2σ (Fig.5d).

*4.2.3. Sample 12GL01*

Only 15 zircon grains were extracted from this sample and 16 U-Pb analyses were performed out of which 9 are concordant at 90–110%. Two grains show Ediacaran dates of 575 ± 21 and 633 ± 22 Ma. Three grains yielded Stenian-late Ectasian dates (at 1.1–1.2 Ga) and four grains Archean dates spanning between 2.6 and 3.3 Ga. In addition, 7 monazite grains were also retrieved from this sample. Seven out of 8 analyses are equivalent (Fig.6b) and allow calculation of a robust Concordia date at 514.6 ± 5.2 Ma ($MSWD_{(C+E)} = 1.07$).

Notably, when all three samples are considered together, zircon date distributions evidence a tendency toward younger ages for the rims (blue) and older ages for the cores (red), both populations recording similar age patterns (Fig.7).

## 5. Discussion

### *5.1. Interpretation of the U—Pb results*

As the investigated xenoliths are interpreted to be metasediments, the new U—Pb dataset can place constraints on the maximal depositional ages of the sedimentary protoliths. Those were calculated based on the robust YC2σ(3+) estimator of Dickinson and Gehrels (2009), i.e. the weighted mean age of the youngest zircon population of at least three grains showing overlapping $^{206}Pb/^{238}U$ dates at 2σ. This approach is particularly suited in the absence of distinctive correlations between zircon date and U content or Th/U ratios, as observed among the Ediacaran populations of samples 12GL02 and 12GL04. Calculated maximal depositional ages are 569.4 ± 5.0 Ma and 575.2 ± 8.3 Ma, respectively (Fig.5c,d). No depositional age was obtained for 12GL01 as only 2 Ediacaran dates were retrieved and do not overlap (Fig.6a). As the enclosing granites are ca. 505 Ma-old, the protoliths of the paragneiss xenoliths are unambiguously of Ediacaran – Lower Cambrian age.

The monazite date of 514.6 ± 5.2 Ma most probably constrains the timing of metamorphism experienced by the xenoliths, before incorporation in the granitic magmas. This age is identical to the Cambrian $^{206}Pb/^{238}U$ date of 514 ± 18 Ma measured on a zircon grain from sample 12GL02, suggesting that this grain possibly (re)crystallized or got its U—Pb system reset during high-grade metamorphism, in agreement with its low Th/U ratio of 0.03 (Rubatto etal., 2001). Metamorphism and plutonic activity at 515–500 Ma can be related to the Ross orogeny (Boger, 2011) which affected several segments of Antarctica and Australia. In that sense, the paragneiss xenoliths of eastern George V Land most probably represent relics of the paleo-Pacific margin of eastern

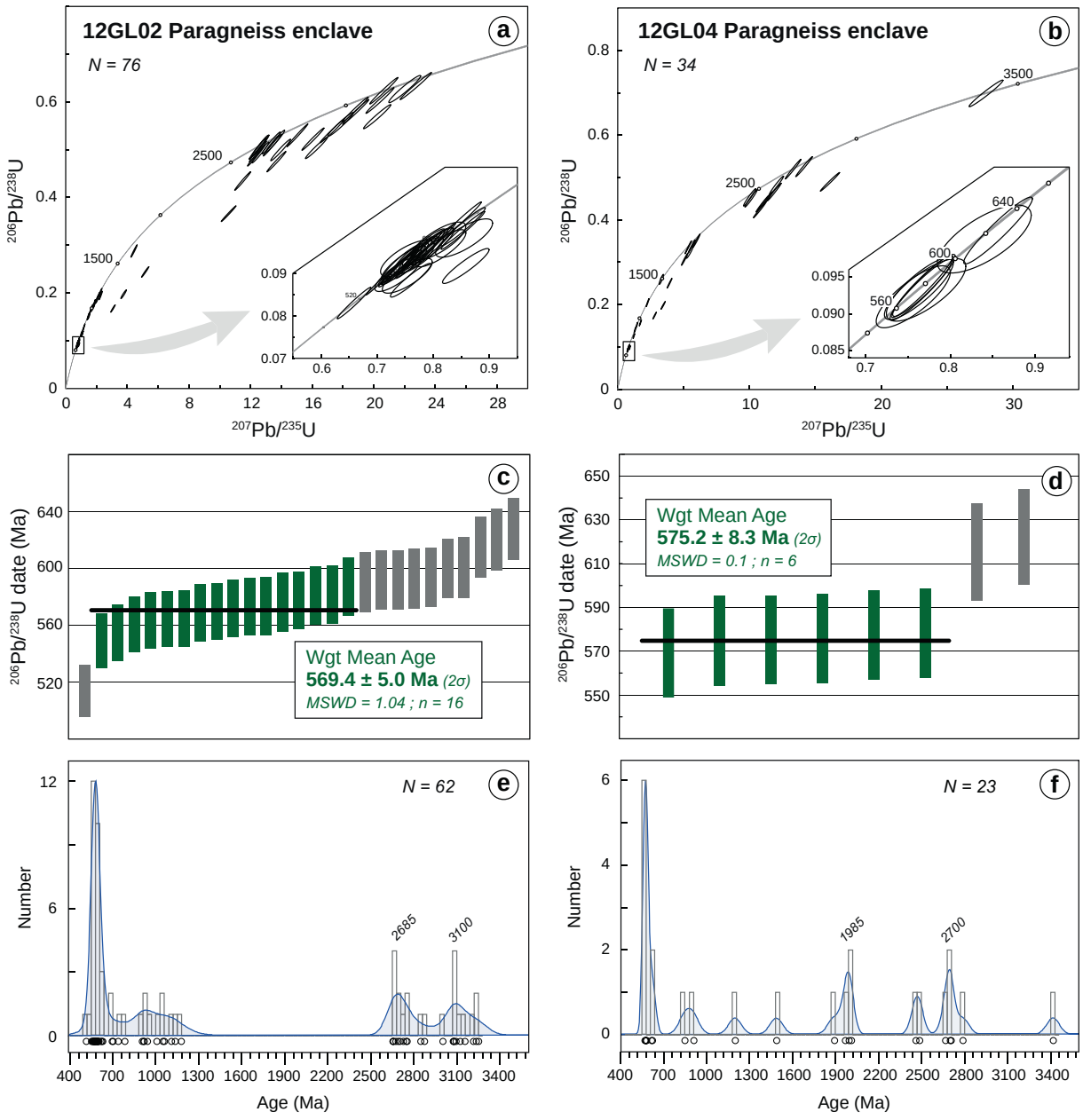


**Fig.5.** Zircon U—Pb results for the East George V Land paragneiss xenoliths 12GL02 and 04. (a,b) Wetherill diagrams. Error ellipses are quoted at 2σ level of uncertainty. (c,d) Average ages calculated for the youngest concordant zircon population following the YC2σ(3+) estimator of Dickinson and Gehrels (2009). (e,f) Zircon U—Pb date distribution represented as Kernel Density Estimates. Only analyses discordant at <10% are displayed. All Kernel Density Estimates were plotted with the Density Plotter program of Vermeesch (2013).

Gondwana that was deformed and metamorphosed during the Ross orogeny.

### 5.2. Relationships between the PBW block and the Terre Adélie-Gawler Cratons

U/Pb ages in the Terre Adélie Craton Paleoproterozoic domain have been published by Peucat etal. (1999). They show (i)that the Dumont d'Urville basin contains two populations of inherited zircon grains bearing SHRIMP ages of about 1.73–1.76, 2.6 and 2.8 Ga and (ii) that a major partial melting event, marked by newly formed zircon and monazite grains, occurred at around 1.69 Ga. In the Neoarchean domain of the Terre Adélie Craton, U—Pb ages were obtained by Oliver etal. (1983); Oliver and Fanning (2002); Ménot (2018). They range between 2.4 and 2.5 Ga and indicate a major period of magmatism and of high grade metamorphism.

Importantly, there is a clear mismatch between the ages recorded in the Terre Adélie craton and the zircon U—Pb date distribution of paragneisses from the PBW block (Fig. 8). In the latter, grains with dates between 1.6 and 1.8 Ga are lacking and only 4 grain domains show dates in the range 2.4–2.6 Ga. A similar conclusion can be drawn when the Gawler craton is considered (Fig.8). These results clearly indicate that the source of older-than-1 Ga zircon grains in the Ediacaran – Lower Cambrian detritus does not originate from the Terre Adélie/Gawler craton. In terms of geodynamic reconstruction, it implies that either (i)an old basement similar to the Terre Adélie/Gawler Cratons is present beneath the PBW block but was not exposed at the time of sediment deposition (Ediacaran to Lower Cambrian) so that it was not reworked as detritus feeding the Ediacaran-Lower Cambrian basins, or (ii) the lack of Terre Adélie/Gawler Cratons signature reflects the presence of a different basement in the PBW block. We favor the second hypothesis because seismic investigations (Lamarque etal., 2015),

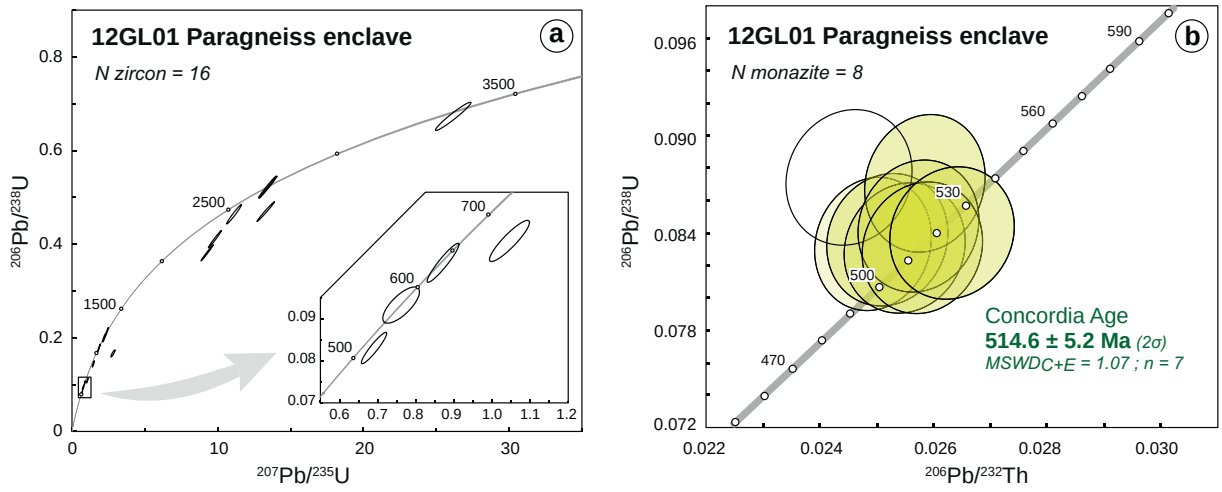


**Fig.6.** Zircon and monazite U-Th-Pb results for the George V Land paragneiss xenolith 12GL01. (a)Wetherill diagram showing zircon U—Pb data. Error ellipses are quoted at 2σ level of uncertainty. (b)$^{206}Pb/^{238}U$ versus $^{208}Pb/^{232}Th$ diagram for the analyzed monazite grains. Error ellipses are quoted at 2σ level of uncertainty.

aeromagnetic exploration (Aitken etal., 2014; Ferraccioli etal., 2009; Finn etal., 2006) and gravity data (Jordan etal., 2013) support that the MSZ is a major continental scale tectonic structure that clearly separates two distinct lithospheric domains of probably contrasted ancestries.

### 5.3. Correlations with South Australia

In order to better constrain the relationships between Antarctica and South Australia before the opening of the Southern Ocean, we attempt to identify the correlative formation(s)of our samples in South Australia. We thus compare in Fig. 9 the detrital zircon U—Pb age distribution of Penguin Point paragneisses to those of the Kanmantoo, Normanville, Adelaidian and Nargoon (meta)sedimentary formations, all deposited in the Ediacaran to Lower Cambrian. From a graphical observation (Fig.9), the zircon U—Pb date distribution of eastern George V Land paragneisses clearly resembles that of the Kanmantoo and Nargoon group sediments. Indeed, they are all characterized by a dominant Ediacaran (≈550–630 Ma) zircon population which is notably lacking in the of Normanville and Adelaidian formations (Fig.9). The latter instead encompass a prominent Mesoproterozoic zircon population not observed in our samples. The match between PBW paragneisses and Kanmantoo/Nargoon sediments is not perfect as: (i)Tonian-Stenian zircon grains are rather scarce in PBW but common to abundant in the Kanmantoo/Nargoon sediments; (ii) the peak at ca. 2.7 Ga typical of the PBW paragneisses is lacking in the Kanmantoo/Nargoon sediments. Because they are of same age (Ediacaran to Lower Cambrian), present a similar zircon date distribution and are (at least for PBW and Kanmantoo) intruded by Paleozoic granitoids formed during the Ross-Delamerian orogeny (see Fig. 1, Di Vincenzo etal., 2007; Foden etal., 2002), we regard the PBW paragneisses as being lateral equivalents to the Kanmantoo/Nargoon sedimentary formations. The above-mentioned discrepancies between their U—Pb date distributions likely reflect lateral variations in the nature of the detritus.

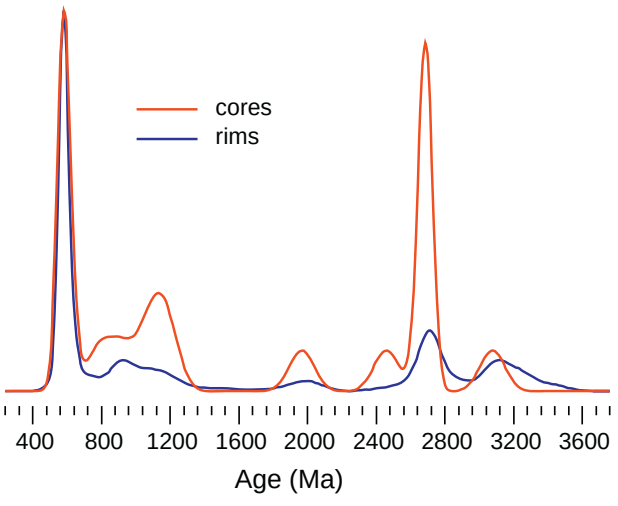


**Fig.7.** U—Pb date distribution of zircon grain cores and rims from all samples, represented as Kernel Density Estimates. Only analyses discordant at <10% are displayed.

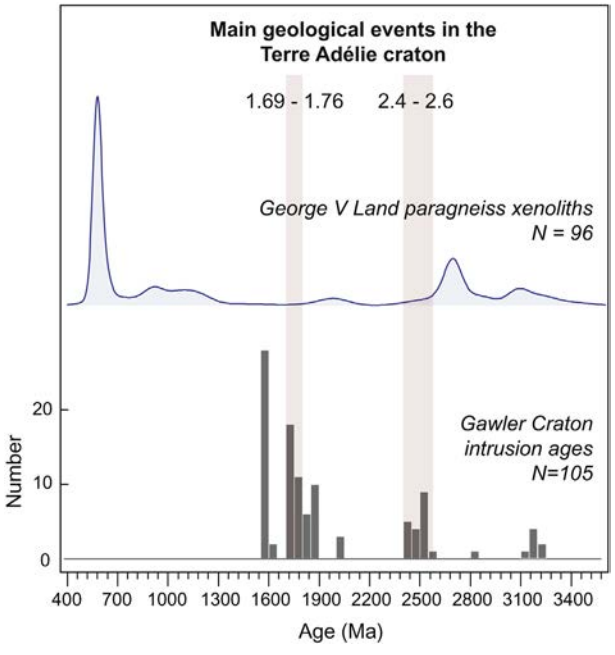


**Fig.8.** Zircon U—Pb date distributions of the George V Land paragneiss xenoliths compared to the main periods of geological activity (magmatism/metamorphism) in the Terre Adélie craton (see text for references and discussion). Is also depicted an histogram summarizing available intrusion ages for the Gawler craton (meta)igneous rocks. For paragneisses zircon data, only analyses discordant at <10% are displayed. Data for the Gawler craton are from the Geochron database of the Australian Geological Survey.

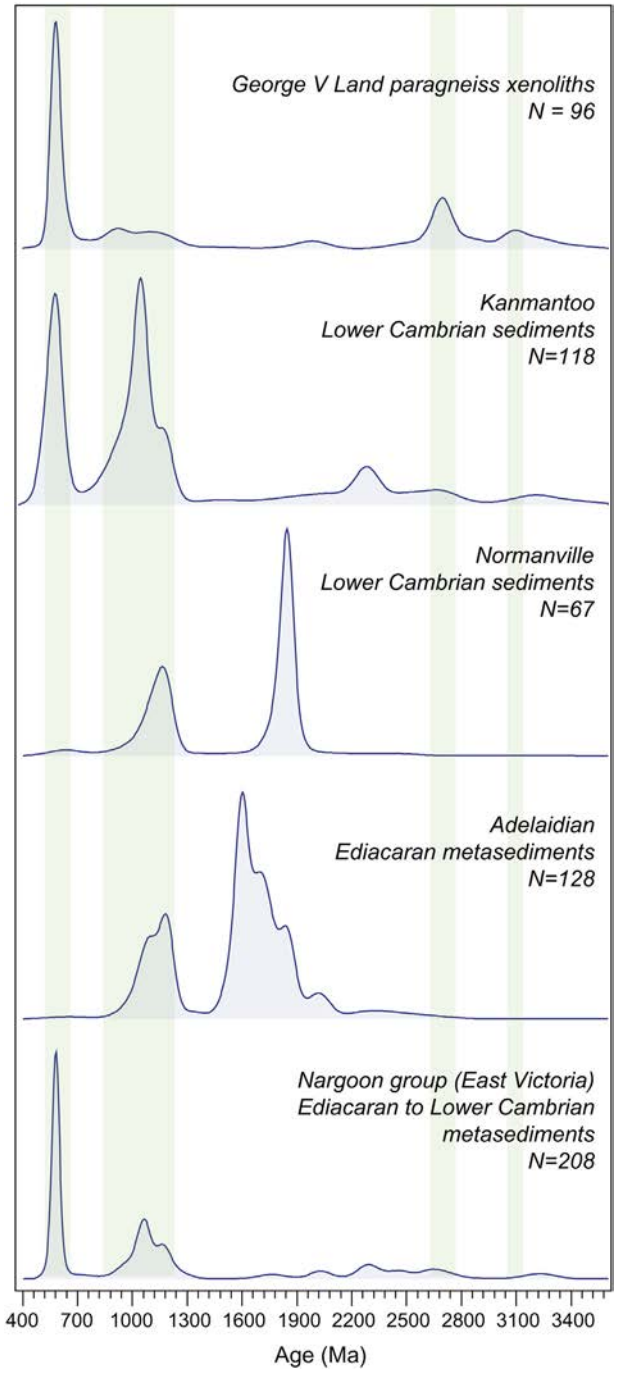


**Fig.9.** Detrital zircon U—Pb date distributions of the George V Land paragneiss xenoliths compared to those of several Ediacaran to Lower Cambrian (meta)sediments from the Delamerian segment of Australia, all represented as Kernel Density Estimates. Only analyses discordant at <10% are displayed. Data sources: Ireland etal. (1998) for Kanmantoo, Normanville and Adelaidian sediments; Geochron database from the Australian Geological Survey for the Nargoon group sediments (East Victoria).

## 6. Conclusion

Zircon and monazite U—Pb dating of paragneisses from the eastern George V Land region reinforces the geological correlations between South Australia and the Terre Adélie-George V Land regions and support the previous geodynamical reconstructions, which were synthetized by Boger (2011). In particular, we have shown that:

(i) Zircon and monazite ages suggest that the studied gneisses are relics of the pre-Gondwana margin, which had been deformed and metamorphosed during the early Paleozoic Ross orogeny.

(ii) Zircon date distributions of the studied samples present strong similarities with the Ediacaran to Lower Cambrian Kanmantoo and Nargoon groups of South Australia, arguing for a correlation between these formations. This has implications for correlations between the east Mertz Shear Zone area in East Antarctica and the eastern terrains of the Gawler Craton in South Australia before the opening of the Southern Ocean.

(iii) There is a clear mismatch between the date distribution of older-than-Mesoproterozoic zircon grains recovered from the paragneisses and the geological record of the adjacent Terre Adélie (and Gawler) cratons. This observation brings into question the actual source of the Paleoproterozoic to Archean detritus that fed the Ediacaran to Lower Cambrian basins of the PBW domain.

Supplementary data to this article can be found online at https://doi.org/10.1016/j.lithos.2018.08.021.

## Acknowledgements

This work was supported by the French Polar Institute (IPEV, Institut Paul Emile Victor) through the programme ArLiTA (Architecture de la Lithosphère de Terre Adélie). ArLiTA also benefited of the support of the INSU-SYSTER programme. Thanks are due to Steven Boger, John Goodge and an anonymous reviewer for their constructive reviews that permit us to greatly improve the document.

## References

Agangi, A., McPhie, J., Kamenetsky, V.S., 2011. Magma chamber dynamics in a silicic LIP revealed by quartz: the Mesoproterozoic Gawler Range Volcanics. Lithos 126: 68–83. https://doi.org/10.1016/j.lithos.2011.06.005.

Aitken, A.R.A., Young, D.A., Ferraccioli, F., Betts, P.G., Greenbaum, J.S., Richter, T.G., Roberts, J.L., Blankenship, D.D., Siegert, M.J., 2014. The subglacial geology of Wilkes Land, East Antarctica. Geophys. Res. Lett. 41:2390–2400. https://doi.org/10.1002/2014GL059405.

Boger, S.D., 2011. Antarctica — before and after Gondwana. Gondwana Res. 19:335–371. https://doi.org/10.1016/j.gr.2010.09.003.

Borg, S.G., DePaolo, D.J., 1994. Laurentia, Australia, and Antarctica as a Late Proterozoic supercontinent: constraints from isotopic mapping. Geology 22, 307–310.

Corfu, F., 1988. Differential response of U-Pb systems in coexisting accessory minerals, Winnipeg River Subprovince, Canadian Shield: implications for Archean crustal growth and stabilization. Contrib. Mineral. Petrol. 98:312–325. https://doi.org/10.1007/BF00375182.

Counts, J.W., 2017. The Adelaide Rift Complex in the Flinders Ranges: Geologic History, Past Investigations and Relevant Analogues. https://doi.org/10.13140/RG.2.2.23216.25609.

Daly, S.J., Fanning, C.M., 1993. Archaean. In: Drexel, J.F., Preiss, W.V., Parker, A.J. (Eds.), The Geology of South Australia, The Precambrian. vol. 1. Geological Survey of South Australia, Adelaide, South Australia, pp. 32–49 Bulletin 54.

Daly, S.J., Fanning, C.M., Fairclough, M.C., 1998. Tectonic evolution and exploration patential of the Gawler Craton, South Australia. J. Aust. Geol. Geophys. 17, 145–168.

Di Vincenzo, G., Talarico, F., Kleinschmidt, G., 2007. An 40Ar/39Ar investigation of the Mertz Glacier area (George V Land, Antarctica): implications for the Ross Orogen–East Antarctic Craton relationship and Gondwana reconstructions. Precambrian Res. 152:93–118. https://doi.org/10.1016/j.precamres.2006.10.002.

Di Vincenzo, G., Grande, A., Rossetti, F., 2014. Paleozoic siliciclastic rocks from northern Victoria Land (Antarctica): Provenance, timing of deformation, and implications for the Antarctica-Australia connection. Geol. Soc. Am. Bull. https://doi.org/10.1130/B31034.1.

Dickinson, W.R., Gehrels, G.E., 2009. Use of U-Pb ages of detrital zircons to infer maximum depositional ages of strata: a test against a Colorado Plateau Mesozoic database. Earth Planet. Sci. Lett. 288:115–125. https://doi.org/10.1016/j.epsl.2009.09.013.

Duclaux, G., Rolland, Y., Ruffet, G., Ménot, R.-P., Guillot, S., Peucat, J.-J., Fanning, M., Rey, P., Pêcher, A., 2008. Superimposed Neoarchaean and paleoproterozoic tectonics in the Terre Adélie Craton (East Antarctica): evidence from Th–U–Pb ages on monazite and 40Ar/39Ar ages. Precambrian Res. 167:316–338. https://doi.org/10.1016/j.precamres.2008.09.009.

Fanning, C.M., Flint, R.B., Parker, A.J., Ludwig, K.R., Blissett, A.H., 1988. Refined proterozoic evolution of the Gawler, South Australia, through U-Pb zircon geochronology. Precambrian Res. 41, 363–386.

Fanning, C., Moore, D.H., Bennett, V., Daly, S., Ménot, R.P., Peucat, J., Oliver, R., 1999. The "Mawson continent": The East Antarctic Shield and Gawler Craton, Australia. 8th International Symposium on Antarctic Earth Sciences, Wellington (New Zealand) (p. 103).

Fanning, C., Ménot, R.P., Peucat, J., Pelletier, A., 2002. A closer examination of the direct links between Southern Australia and Terre Adélie and George V Land, Antarctica. 16th Australian Geological Convention. Adelaide.
Fanning, C.M., Peucat, J.J., Ménot, R.P., 2003. Whither the Mawson continent? 9th International Symposium on Antarctic Earth Sciences. Potsdam
Fanning, C.M., Reid, A.J., Teale, G.S., 2007. A Geochronological Framework for the Gawler Craton. South Australia, South Australia Geological Survey Bulletin.
Ferraccioli, F., Armadillo, E., Jordan, T., Bozzo, E., Corr, H., 2009. Aeromagnetic exploration over the East Antarctic Ice Sheet: a new view of the Wilkes Subglacial Basin. Tectonophysics 478:62–77. https://doi.org/10.1016/j.tecto.2009.03.013.
Finn, C.A., Goodge, J.W., Damaske, D., Fanning, C.M., 2006. Scouting craton's edge in paleo-Pacific Gondwana. Antarctica: Contributions to Global Earth Sciences. Berlin Heidelburg New York, pp. 165–174.
Fitzsimons, I.C.W., 2003. Proterozoic basement provinces of southern and southwestern Australia, and their correlation with Antarctica. Geol. Soc. Lond. Spec. Publ. 206: 93–130. https://doi.org/10.1144/GSL.SP.2003.206.01.07.
Flöttmann, T., Gibson, G.M., Kleinschmidt, G., 1993. Structural continuity of the Ross and Delamerian orogens of Antarctica and Australia along the margin of the paleo-Pacific. Geology 21, 319–322.
Foden, J.D., Elburg, M.A., Turner, S.P., Sandiford, M., O'Callaghan, J., Mitchell, S., 2002. Granite production in the Delamerian Orogen, South Australia. J. Geol. Soc. 159:557–575. https://doi.org/10.1144/0016-764901-099.
Forbes, B.G., Murrell, B., Preiss, W.V., 1981. Sudbivision of Lower Adelaidean Willouran Ranges.
Fraser, G., McAvaney, S., Neumann, N., Szpunar, M., Reid, A., 2010. Discovery of early Mesoarchean crust in the eastern Gawler Craton, South Australia. Precambrian Res. 179:1–21. https://doi.org/10.1016/j.precamres.2010.02.008.
Gasquet, D., Bertrand, J., Paquette, J., Lehmann, J., Ratzov, G., De Ascenção Guedes, R., Tiepolo, M., Boullier, A., Scaillet, S., Nomade, S., 2010. Miocene to Messinian deformation and hydrothermalism in the Lauzière Massif (French Western Alps): new U-Th-Pb and Argon ages. Bull. Soc. Geol. Fr. 181, 227–241.
Gibson, G.M., Totterdell, J.M., White, L.T., Mitchell, C.H., Stacey, A.R., Morse, M.P., Whitaker, A., 2013. Pre-existing basement structure and its influence on continental rifting and fracture zone development along Australia's southern rifted margin. J. Geol. Soc. 170: 365–377. https://doi.org/10.1144/jgs2012-040.
Goodge, J.W., Fanning, C.M., 2010. Composition and age of the East Antarctic Shield in eastern Wilkes Land determined by proxy from Oligocene-Pleistocene glaciomarine sediment and Beacon Supergroup sandstones, Antarctica. Geol. Soc. Am. Bull. 122: 1135–1159. https://doi.org/10.1130/B30079.1.
Haines, P.W., Turner, S.P., Foden, J.D., Jago, J.B., 2009. Isotopic and geochemical characterisation of the Cambrian Kanmantoo Group, South Australia: implications for stratigraphy and provenance. Aust. J. Earth Sci. 59, 1095–1110.
Hanchar, J.M., Miller, C.F., 1993. Zircon zonation patterns as revealed by cathodoluminescence and backscattered electron images: implications for interpretation of complex crustal histories. Chem. Geol. 110:1–13. https://doi.org/10.1016/0009-2541(93)90244-D.
Hand, M., Reid, A., Jagodzinski, L., 2007. Tectonic framework and evolution of the Gawler Craton, Southern Australia. Econ. Geol. 102:1377–1395. https://doi.org/10.2113/gsecongeo.102.8.1377.
Howard, K.E., Reid, A.J., Hand, M.P., Barovich, K.M., Belousova, E.A., 2006. Does the Kalinjala Shear Zone represent a palaeosuture zone? Implications for distribution of styles of Mesoproterozoic mineralisation in the Gawler Craton. Earth 16–20.
Howard, K.E., Hand, M., Barovich, K.M., Reid, A., Wade, B.P., Belousova, E.a., 2009. Detrital zircon ages: improving interpretation via Nd and Hf isotopic data. Chem. Geol. 262: 293–308. https://doi.org/10.1016/j.chemgeo.2009.01.029.
Hurai, V., Paquette, J.L., Huraiová, M., Konečnỳ, P., 2010. U-Th-Pb geochronology of zircon and monazite from syenite and pincinite xenoliths in Pliocene alkali basalts of the intra-Carpathian back-arc basin. J. Volcanol. Geotherm. Res. 198:275–287. https://doi.org/10.1016/j.jvolgeores.2010.09.012.
Ireland, T.R., Flöttmann, T., Fanning, C.M., Gibson, G.M., Preiss, W.V., 1998. Development of the early Paleozoic Pacific margin of Gondwana from detrital-zircon ages across the Delamerian orogen. Geology 26:243–246. https://doi.org/10.1130/0091-7613(1998)026<0243.
Jackson, S.E., Pearson, N.J., Griffin, W.L., Belousova, E.A., 2004. The application of laser ablation-inductively coupled plasma-mass spectrometry to in situ U-Pb zircon geochronology. Chem. Geol. 211:47–69. https://doi.org/10.1016/j.chemgeo.2004.06.017.
Jordan, T.A., Ferraccioli, F., Armadillo, E., Bozzo, E., 2013. Crustal architecture of the Wilkes Subglacial Basin in East Antarctica, as revealed from airborne gravity data. Tectonophysics 585:196–206. https://doi.org/10.1016/j.tecto.2012.06.041.
Kleinschmidt, G., Talarico, F., 2000. The Mertz shear zone. Terra Antarct. Rep. 5, 109–115.
Knoll, A.H., Walter, M.R., Narbonne, G.M., Christie-Blick, N., 2006. The Ediacaran period: a new addition to the geologic time scale. Lethaia 39:13–30. https://doi.org/10.1080/00241160500409223.
Kohn, M.J., Vervoort, J.D., 2008. U-Th-Pb dating of monazite by single-collector ICP-MS: pitfalls and potential. Geochem. Geophys. Geosyst. 9. https://doi.org/10.1029/2007GC001899.
Krieg, G.W., Rogers, P.A., Callen, R.A., Freeman, P.J., Alley, N.F., Forbes, B.G., 1991. Curdimurka, South Australia.
Lamarque, G., Barruol, G., Fontaine, F.R., Bascou, J., Ménot, R.-P., 2015. Crustal and mantle structure beneath the Terre Adelie Craton, East Antarctica: insights from receiver function and seismic anisotropy measurements. Geophys. J. Int. 200:809–823. https://doi.org/10.1093/gji/ggu430.
Lamarque, G., Bascou, J., Maurice, C., Cottin, J.-Y., Riel, N., Ménot, R.-P., 2016. Microstructures, deformation mechanisms and seismic properties of a Palaeoproterozoic shear zone: the Mertz shear zone, East-Antarctica. Tectonophysics 680:174–191. https://doi.org/10.1016/j.tecto.2016.05.011.
Lewis, C.J., Cayley, R.A.R.J., Schofield, A., Taylor, D.H., 2016. New SHRIMP U-Pb zircon ages from the Stavely region, western Victoria: July 2014–June 2016. Geoscience Australia.
Ludwig, K., 2008. User's manual for Isoplot Version 3.70, a geochronological toolkit for Microsoft Excel. Berkeley Geochronology Center Special Publications. 4, pp. 1–76.
McLean, M.A., Betts, P.G., 2003. Geophysical constraints of shear zones and geometry of the Hiltaba Suite granites in the western Gawler Craton, Australia. Aust. J. Earth Sci. 50:525–541. https://doi.org/10.1046/j.1440-0952.2003.01010.x.
Ménot, R.P., 2018. East antarctica. In: Kleinschmidt, G. (Ed.), Geology of the Antarctic Continent. Schweizerbart Plut, Stuttgart.
Ménot, R., Pêcher, A., Rolland, Y., Peucat, J., Pelletier, A., Duclaux, G., Guillot, S., 2005. Structural setting of the Neoarchean Terrains in the Commonwealth Bay Area (143-145°E), Terre Adélie Craton, East Antarctica. Gondwana Res. 8, 1–9.
Ménot, R.P., Duclaux, G., Peucat, J.J., Rolland, Y., Guillot, S., Fanning, M., Bascou, J., Gapais, D., Pêcher, A., 2007. Geology of the Terre Adélie Craton (135–146°E ), East Antarctica. In: Cooper, A., Raymond, C., Al, E. (Eds.), Antarctica: A Keystone in a Changing World - Online Proceedins for the Tenth International Symposium on Antarctica Earth Sciences. USGS Open-file Report 2007–1047 https://doi.org/10.3133/of2007-1047.srp048 (extended Abstract, p. 1047).
Milnes, A.R., Compston, W., Daily, B., 1977. Pre- to syn-tectonic emplacement of early palaeozoic granites in southeastern South Australia. J. Geol. Soc. Aust. 24, 87–106.
Oliver, R., Fanning, C., 1997. Australia and Antarctica: Precise correlation of Paleoproterozoic terrains. The Antarctic Region: Geological Evolution and Processes, pp. 163–172.
Oliver, R., Fanning, C., 2002. Proterozoic geology east and southeast of Commonwealth Bay, George V Land, Antarctica, and its relationship to that of adjacent Gondwana terranes. Antarctica at the Close of the Millenium. 35. Royal Society of New Zealand, Bulletin, pp. 51–58.
Oliver, R., Cooper, J.A., Truelove, A.J., 1983. Petrology and zircon geochronology of Herring Island and Commonwealth Bay and Evidence for Gondwana Reconstruction. Antarctic Earth Science, pp. 64–68.
Parker, A.J., 1980. The Kalinjala Mylonite Zone, eastern Eyre Peninsula. South Australia. Geological Survey. Quarterly Geological Notes, pp. 6–11.
Paquette, J.L., Piro, J.L., Devidal, J.L., Bosse, V., Didier, A., 2014. Sensitivity enhancement in LA-ICP-MS by N2 addition to carrier gas: application to radiometric dating of U-Th-bearing minerals. Agilent ICP-MS J. 58, 4–5.
Paquette, J.L., Ballèvre, M., Peucat, J.J., Cornen, G., 2017. From opening to subduction of an oceanic domain constrained by LA-ICP-MS U-Pb zircon dating (Variscan belt, Southern Armorican Massif, France). Lithos 294–295:418–437. https://doi.org/10.1016/j.lithos.2017.10.005.
Parker, A.J., Lemon, N.M., 1982. Reconstruction of the Early Proterozoic stratigraphy of the Gawler Craton, South Australia. J. Geol. Soc. Aust. 29:221–238. https://doi.org/10.1080/00167618208729206.
Payne, J.L., Hand, M., Barovich, K.M., Reid, A., Evans, D.A.D., 2009. Correlations and reconstruction models for the 2500-1500 Ma evolution of the Mawson Continent. Geol. Soc. Lond. Spec. Publ. 323:319–355. https://doi.org/10.1144/SP323.16.
Payne, J.L., Ferris, G., Barovich, K.M., Hand, M., 2010. Pitfalls of classifying ancient magmatic suites with tectonic discrimination diagrams: an example from the Paleoproterozoic Tunkillia Suite, southern Australia. Precambrian Res. 177:227–240. https://doi.org/10.1016/j.precamres.2009.12.005.
Pelletier, A., Guiraud, M., Menot, R.-P., 2005. From partial melting to retrogression in the Pointe Geologie migmatitic complex: a history of heterogeneous distribution of fluids. Lithos 81:153–166. https://doi.org/10.1016/j.lithos.2004.10.003.
Peucat, J.J., Ménot, R.P., Monnier, O., Fanning, C., 1999. The Terre Adélie basement in the East-Antarctica Shield: geological and isotopic evidence for a major 1.7 Ga thermal event; comparison with the Gawler Craton in South Australia. Precambrian Res. 94, 205–224.
Peucat, J.J., Capdevila, R., Fanning, C.M., Ménot, R.P., Pécora, L., Testut, L., 2002. 1.60 Ga felsic volcanic blocks in the moraines of the Terre Adélie Craton, Antarctica: comparisons with the Gawler Range Volcanics, South Australia. Aust. J. Earth Sci. 49, 831–845.
Ravich, M.G., Klimov, L.V., Solov'ev, D.S., 1968. The Pre-Cambrian of the East Antarctica. Isreal Program for Scientific Translations Ltd, Jerusalem (translation of Ravich et al., 1965).
Reading, A.M., 2004. The Seismic Structure of Wilkes Land/Terre Adelie, East Antarctica and Comparison with Australia: first steps in Reconstructing the Deep Lithosphere of Gondwana. Gondwana Res. 7:21–30. https://doi.org/10.1016/S1342-937X(05)70303-8.
Reid, A.J., Hand, M., 2012. Mesoarchean to mesoproterozoic evolution of the southern Gawler Craton, South Australia. Episodes 35, 216–225.
Reid, A.J., Jagodzinski, E.a., Armit, R.J., Dutch, R.a., Kirkland, C.L., Betts, P.G., Schaefer, B.F., 2014. U-Pb and Hf isotopic evidence for Neoarchean and Paleoproterozoic basement in the buried northern Gawler Craton, South Australia. Precambrian Res. 250: 127–142. https://doi.org/10.1016/j.precamres.2014.05.019.
Rubatto, D., Williams, I.S., Buick, I.S., 2001. Zircon and monazite response to prograde metamorphism in the Reynolds Range, central Australia. Contrib. Mineral. Petrol. 140:458–468. https://doi.org/10.1007/PL00007673.
Swain, G., Barovich, K., Hand, M., Ferris, G., Schwarz, M., 2008. Petrogenesis of the St Peter Suite, southern Australia: Arc magmatism and Proterozoic crustal growth of the South Australian Craton. Precambrian Research, Assembling Australia: Proterozoic building of a continent 166, 283–296. https://doi.org/10.1016/j.precamres.2007.07.028.
Swain, G., Hand, M., Teasdale, J., Rutherford, L., Clark, C., 2005. Age constraints on terrane-scale shear zones in the Gawler Craton, southern Australia. Precambrian Res. 139: 164–180. https://doi.org/10.1016/j.precamres.2005.06.007.
Talarico, F., Kleinschmidt, G., 2003a. The Mertz Shear Zone (George V Land): Implications for Australia/Antarctica Correlations and East Antarctic Craton/Ross Orogen Relationships. Terra Antarct. Rep. 9, 149–153.

Talarico, F., Kleinschmidt, G., 2003b. Structural an metamorphic evolution of the Mertz Shear Zone (East Antarctic Craton, Geroge V Land): implications for Australia/Antarctica correlations and East Antarctic craton/Ross Orogen relationships. Terra Antarct. 10, 229–248.

Van Achterbergh, E., Ryan, C., Jackson, S., Griffin, W., 2001. Data reduction software for LA-ICP-MS. Laser Ablation-ICPMS in the Earth Science. Mineralogical Association of Canada, pp. 239–243.

Vassallo, J.J., Wilson, C.J.L., 2002. Palaeoproterozoic regional-scale non-coaxial deformation: an example from eastern Eyre Peninsula, South Australia. J. Struct. Geol. 24: 1–24. https://doi.org/10.1016/S0191-8141(01)00043-8.

Vavra, G., 1990. On the kinematics of zircon growth and its petrogenetic significance: a cathodoluminescence study. Contrib. Mineral. Petrol. 106:90–99. https://doi.org/10.1007/BF00306410.

Vermeesch, P., 2004. How many grains are needed for a provenance study? Earth Planet. Sci. Lett. 224:441–451. https://doi.org/10.1016/j.epsl.2004.05.037.

Vermeesch, P., 2012. On the visualisation of detrital age distributions. Chem. Geol. 312–313:190–194. https://doi.org/10.1016/j.chemgeo.2012.04.021.

Vermeesch, P., 2013. Multi-sample comparison of detrital age distributions. Chem. Geol. 341:140–146. https://doi.org/10.1016/j.chemgeo.2013.01.010.

Wiedenbeck, M., Allé, P., Corfu, F., Griffin, W.L., Meier, M., Oberli, F., von Quadt, A., Roddick, J.C., Spiegel, W., 1995. Three natural zircon standards for U-Th-Pb, Lu-Hf, trace element and Ree analyses. Geostand. Geoanal. Res. 19:1–23. https://doi.org/10.1111/j.1751-908X.1995.tb00147.x.

Zang, W.-L., Jago, J.B., Alexander, E.M., Paraschivoiu, E., 2004. A review of basin evolution, sequence analysis and petroleum potential of the frontier Arrowie Basin, South Australia. Special Publication. In: Boult, P.J., Johns, D.R., Lang, S.C. (Eds.), Eastern Australasian Basins Symposium II. Adelaide Petroleum Exploration Society of Australia, pp. 243–256.